



Technical Report 2026
September 2013

Characterization of Coupled Coil in Seawater for Wireless Power Transfer

A NISE funded Applied Research Project

Viktor Bana
Greg Anderson
Lu Xu
Doeg Rodriguez
Alex Phipps
John D. Rockway

Approved for public release.

SSC Pacific
San Diego, CA 92152-5001

SSC Pacific
San Diego, California 92152-5001

J. J. Beel, CAPT, USN
Commanding Officer

C. A. Keeney
Executive Director

ADMINISTRATIVE INFORMATION

This report was prepared for the Office of Naval Research (ONR) by the ISR/IO Department (Code 56), SPAWAR Systems Center Pacific, San Diego, CA. The project is funded by the Naval Innovative Science and Engineering (NISE) Program as an Applied Research project.

Released by
J. Spenser, Head
Radiation Technologies Branch

Under authority of
J. Dombrowski, Acting Head
Maritime Systems Division

This is a work of the United States Government and therefore is not copyrighted. This work may be copied and disseminated without restriction.

EXECUTIVE SUMMARY

This report presents the electrical characterization of coupled electromagnetic coils in saltwater for an undersea wireless power transfer system. The resonant frequency of the system, as well as the separation gap between coils, was varied in both air and seawater to study the effects of saltwater on the energy transfer process. The results indicate that wireless power transfer can be achieved for *in situ* charging of unmanned vehicles in the ocean.

CONTENTS

EXECUTIVE SUMMARY	1
1. INTRODUCTION	2
2. UNDERSEA WIRELESS POWER TRANSFER SYSTEM	2
2.1 IMPEDANCE OF A SINGLE-COIL IN SEAWATER.....	3
2.2 MUTUAL INDUCTANCE BETWEEN COILS IN SEAWATER.....	5
3. DESIGN OF RF COILS	6
4. INPUT IMPEDANCE MEASUREMENTS	7
4.1 SINGLE-COIL MEASUREMENTS	8
4.2 COUPLED TWO-COIL MEASUREMENTS.....	10
5. CONCLUSION	12
6. REFERENCES	12

Figures

1. (a) Circuit diagram for a two-coil Y Δ model, and (b) an equivalent Δ model	1
2. Comparison of the resistances for a coil in air and saltwater. The red dashed line (--) and dotted line (:) is the AC and DC resistance, respectively. The solid red line (-) is the radiation resistance of the loop in air. The solid blue line is the radiation resistance of the loop in seawater	4
3. Comparison of the inductance for a coil in air and saltwater. The red solid line (-) and dotted line (:) is the inductance of a coil in air given by the above formula and Grover's equation. The solid blue line (-) is the inductance of the coil in seawater.....	5
4. Mutual inductance of a coil in a conductive medium. Comparison of the inductance for a coil in air and saltwater. The red solid lines (-) are the inductance of a coil in air given by Grover's equation. The dashed lines (-) in blue are the inductances of the coil in seawater.....	6
5. a) Tethered circular coil (left), and b) solenoid coils (right)	7
6. Experimental setup for two-coil measurements in a seawater tank	8
7. Input impedance measurements versus frequency for a single cylindrical coil in air and seawater, (a) resistance, and (b) reactance	9
8. Quality factor of the coils in air, seawater, and atop a ferrite plate	9
9. Input impedance measurement versus frequency for the transmit solenoid in air and seawater, (a) resistance, and (b) reactance	10
10. Comparison of the input impedance versus frequency for coupled cylindrical coils in air versus saltwater. Measurements are conducted for difference spacing between coils.....	11

11. Comparison of the input impedance versus frequency for the coupled transmit and receive solenoid in air versus saltwater. Measurement was performed for the receive coil slotted inside the transmit coil	11
12. Separation coefficient for cylindrical coils ('blue'). quality factor of the coils in air, seawater, and atop a ferrite plate	12

1. INTRODUCTION

A key challenge to undersea unmanned vehicle (UUV) operations is the finite mission duration times that result primarily from limitations in power storage. Due to the autonomous nature of these vehicles, UUVs are power limited by both space constraints and physical distance from external energy sources. Consequently, UUVs must constantly be extracted from the ocean, serviced (e.g., battery replaced), and then re-deployed, resulting in unwanted lapses in operations. To increase the longevity of these systems, the vehicles must be recharged in situ. The two techniques currently used to recharge UUVs without extraction implement either an electric socket or rotary transformer [1, 2]. Unfortunately, both of these techniques require precision mating for the transfer of electrical energy. For the electrical socket configuration, any physical misalignments can lead to shorting or corrosion of the conductors used in the power transfer. While the rotary transformer approach addresses issues with exposed conductors, alignment on the order of millimeters is required for efficient power transfer. In practice, this degree of alignment is difficult to achieve for deployed underwater systems.

An alternative approach to the electrical socket and rotary transformer is to adopt wireless power transfer (WPT) technology being developed in the commercial sector and adapt it to the underwater maritime environment. There are several key advantages to implementing this type of WPT. First, WPT is designed to transmit power over larger distances (>centimeters) without direct contact, and transfer efficiency is relatively high (>75%). However, several open-ended questions must be answered to transfer power in an underwater operational environment. Eddy current losses, for example, caused by inductive power transfer through a conductive medium (i.e., the ocean), will have detrimental effects on the efficiency of the power transfer. Additional losses associated with the skin effect will also reduce efficiency.

To better understand these and other issues associated with Y RV through ugc y cvgt. 'j k' y qtm investigates the electromagnetic properties of coils that will be exposed to the qegcp0Htuv. 'j g impedance of a single coil in seawater is analyzed and compared to the impedance of c"eqkikp"ckt0. An analysis is then presented for the mutual inductance between two coils in seawater. Input impedance measurements are then performed on single coils submerged in saltwater. From these impedance measurements, the resistance, inductance, and quality factor, Q, for the single-coil systems are extracted. The change in these electrical properties for coils in air versus seawater is also examined. Input impedance measurements are then made for coupled sets of two coils, in both air and seawater. The coupling coefficient is extracted from these measurements. The studies performed here provide an explanation on the effects the saltwater channel would have on the coil's electrical properties and coupling mechanics. The analysis will show that there is an upper frequency bound of operation in seawater. Finally, it demonstrates that the operating frequency of coil system in seawater is approximately 100 kHz, which is comparable in performance to power transfer through air.

2. UNDERSEA WIRELESS POWER TRANSFER SYSTEM

The circuit diagram [3, 4] in Figure 1(a) is a possible schematic of a wireless power transfer system. The coils, both the transmitter and receiver, can be represented by an inherent inductance, L , and inherent resistance, R . The load resistance is represented by Z_L . For the coil to resonate at the desired frequency

of operation, ω , a capacitor, C , is placed in series with the coil. Finally, the coil coupling is represented by the mutual inductance, M .

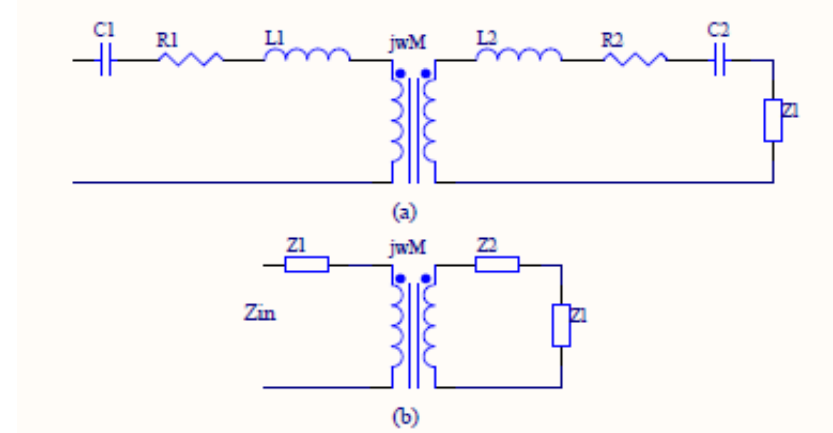


Figure 1. (a) Circuit diagram for a two-coil WPT, and (b) equivalent input impedance model.

The two-coil WPT system can be further simplified, and is characterized by an equivalent input impedance model, shown in Figure 1(b). The input impedance as seen by the transmit coil, Z_{in} , is

$$Z_{in} = Z_1 + \frac{\omega^2 M^2}{Z_2 + Z_L}.$$

The input impedance expression captures the system coupling (M), load impedance (ZL), and the impedances of each coil (Z1 and Z2), where Z1 is the impedance of the transmit coil, and Z2 is the impedance of the receive coil. The impedance for each coil is given by

$$Z = R + j\omega L + 1/j\omega C.$$

In this work, it is assumed that saltwater will modify the electrical characteristics of the coils. To test this assumption, single-coil and coupled two-coil systems are examined. Any additional losses (resistances) or changes in reactance (inductance) because of saltwater are recorded.

2.1 IMPEDANCE OF A SINGLE COIL IN SEAWATER

Many different authors [6, 7] have studied the impedance of a single loop in a conductive medium. For instance, Kraichman developed expressions for the change in radiation resistance and reactance for a thinly insulated circular loop in a conductive medium. Here, these formulas are examined for coils immersed in seawater and compared it to coils in air.

The total resistance of a coil in air or seawater is

$$R = R_{DC} + R_{AC} + R_{rad},$$

where R_{DC} is the DC resistance dependent upon conductor size, R_{AC} is resistance due to skin depth, and R_{rad} is the radiation resistances. The DC and AC resistances for a coil in air or saltwater will be similar in magnitude, since these resistance are based on the type of wire and how it is wound. The radiation resistance for a loop in a conductive medium was derived by Kraichman [5] and is given by

$$R_{rad}^{sea} = \omega \mu a \left[\frac{4}{3}(\beta a)^2 - \frac{\pi}{3}(\beta a)^3 + \frac{2\pi}{15}(\beta a)^5 - \dots \right],$$

where a is the radius of the loop in meters, μ is the permeability of medium, ω is the frequency in radians, σ is the conductivity of medium, c is the speed of light, and $\beta = (\mu\omega\sigma/2)^{1/2}$. In comparison, the radiation resistance of the coil in free space is given by the well-known formula [6]:

$$R_{rad}^{air} = \frac{\pi}{6} \frac{\omega^4 \mu a^4}{c^3}.$$

Figure 2 shows a comparison of the calculated DC and AC resistances of a coil used for experimental tests. Also included are plots of the radiation resistance of a coil in both air and saltwater. The coil is 6 cm in radius with 15 turns. The permittivity and conductivity of the ocean is approximated as $\epsilon_r = 72$ and $\sigma = 4$ S/m. The radiation resistance of the coil in air is negligible. By comparison, the radiation resistance of the coil in seawater, at frequencies greater than 150 kHz, increases more rapidly with frequency than the AC resistance, which normally dominates the losses in air.

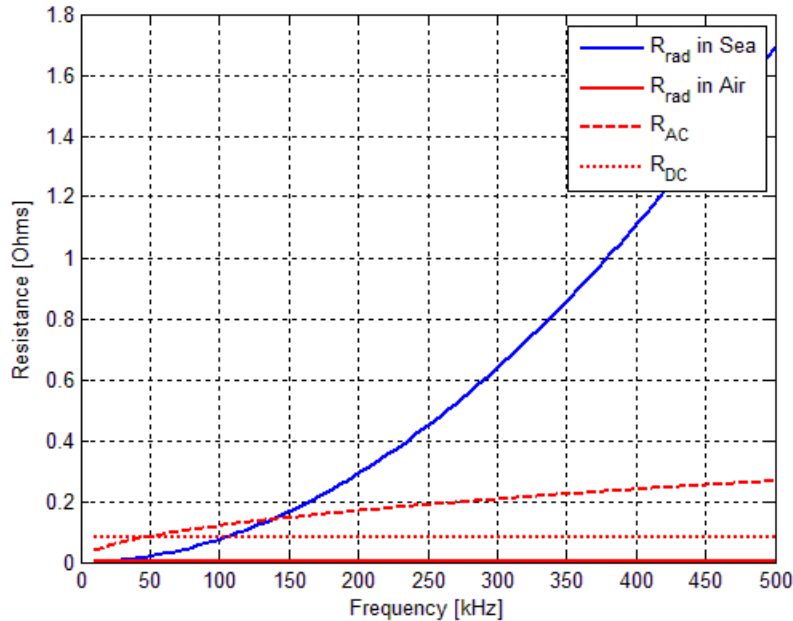


Figure 2. Comparison of the resistances for a coil in air and saltwater. The red dashed line (--) and dotted line (:) is the AC and DC resistance, respectively. The solid red line (-) is the radiation resistance of the loop in air. The solid blue line is the radiation resistance of the loop in seawater.

Kraichman also derived an expression for the reactance of a loop in seawater [6]:

$$X = \omega \mu a \left[K(k) - 2 - \frac{\pi}{3}(\beta a)^3 + \frac{4}{15}(\beta a)^4 - \dots \right],$$

where $K(k)$ is the complete elliptic integral of the first kind. In comparison, the reactance of a single-turn coil in air is given by

$$X_{air} = \omega \mu a [K(k) - 2].$$

Substituting the reactance in air into the reactance of the coil in the conductive media yields

$$X = X_{air} - \omega \mu a \left[\frac{\pi}{3} (\beta a)^3 - \frac{4}{15} (\beta a)^4 - \dots \right].$$

Figure 3 shows a comparison of the calculated inductance for the same coil located in air ('red') and in seawater ('blue') as a function of frequency. The inductance is determined from the above expressions for reactance. Also included is Grover's inductance calculation for a circular loop [7]. A key finding of this study is that the difference in inductance of a coil in air or submerged in seawater from 10 kHz to 1 MHz is less than 4%.

The current analysis shows seawater has an effect on the resistances of a coil. This depends on the coil geometry, size, and operational frequency. Higher frequencies lead to worse losses. In contrast, the effect of operational frequency on the inductance of the coils is nominal.

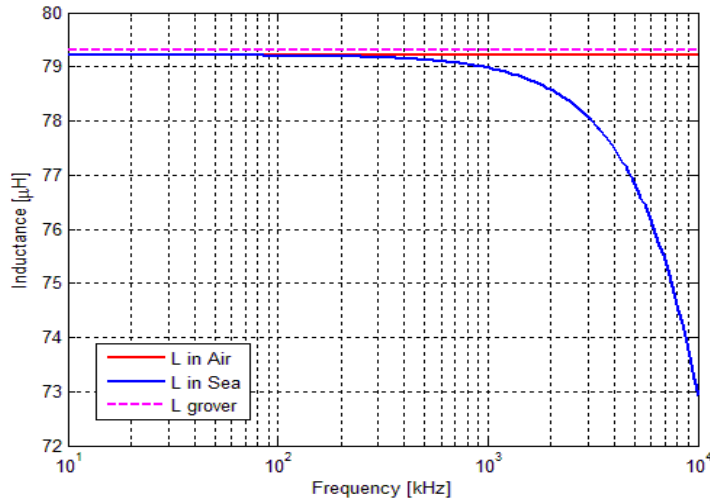


Figure 3. Comparison of the inductance for a coil in air and saltwater. The red solid line (-) and dotted line (:) is the inductance of a coil in air given by the above formula and Grover's equation. The solid blue line (-) is the inductance of the coil in seawater.

2.2 MUTUAL INDUCTANCE BETWEEN COILS IN SEAWATER

For a two-coil system, the mutual inductance between two tightly wound, thin circular coils co-axial located and separated by a distance, d , is given by Grover's formula [7]:

$$M = \mu N_1 N_2 \sqrt{R_1 R_2} \left\{ \left(\frac{2}{k} - k \right) K(k) - \frac{2}{k} E(k) \right\},$$

where μ is the permeability of the medium, N_1 and N_2 are the number of turns of the two coils, $k = 4R_1 R_2 / ((R_1 + R_2)^2 + d^2)$, d is the spacing between coils, R_1 is the radius of coil one, R_2 is the radius of coil 2, and $K(k)$ and $E(k)$ are the elliptical integrals of the first and second kind. The relative permeability of air or free-space is the same for saltwater ($\mu_r = 1$). Therefore, the mutual coupling between coils is not going to change significantly, whether in air or saltwater.

The mutual inductance is derived while assuming the medium is dissipative. While this is true at lower frequencies, this approximation is not satisfied in seawater at higher frequencies. To understand the high-frequency cut-off of coils in seawater, we can remove the quasi-static approximation to

Neumann's original formula. Starting with Neumann's formula and including full-wave affects [8], the mutual inductance is

$$M_{21} = \mu \oint_{Loop2} \oint_{Loop1} \frac{e^{-jk|\mathbf{r}-\mathbf{r}'|} d\mathbf{l}_1 \bullet d\mathbf{l}_2}{4\pi |\mathbf{r} - \mathbf{r}'|}.$$

Figure 4 is a comparison of the mutual inductance between two coils versus frequency in air using Grover's formula ('solid') and seawater ('dash') using the above expression. Two different coil cases were considered. The first case was for coil geometry and spacing, $R_1 = R_2 = d = 6$ cm. The second case was for $R_1 = R_2 = d = 15$ cm. In the 6-cm case, variation was smaller in mutual inductance over a 30-kHz to 1-MHz frequency. However, variation was greater in mutual inductance in seawater versus air for the 15-cm case. For instance, variation was 11% in mutual inductance at 400 kHz. For different coil geometries and spacing, disparity must be considerable in the mutual inductance between coils in seawater versus air.

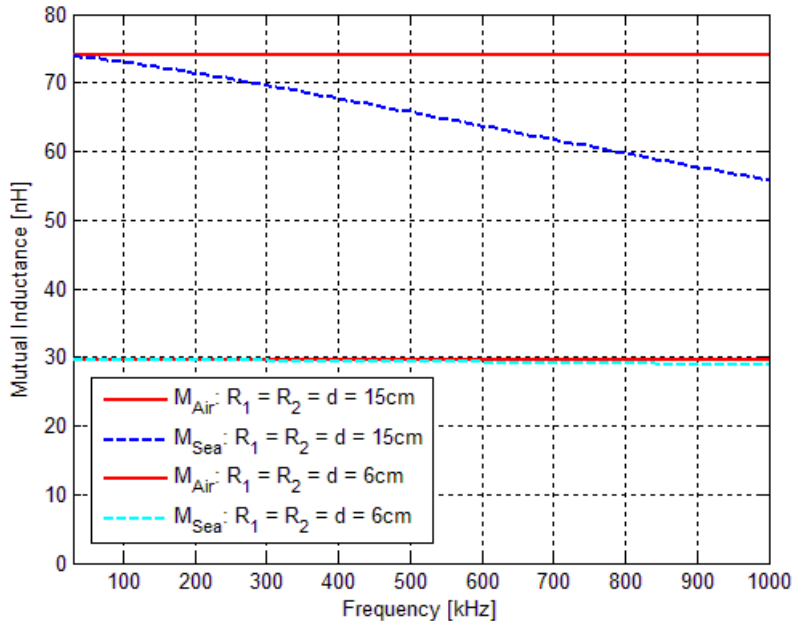


Figure 4. Mutual inductance of a coil in a conductive medium. Comparison of the inductance for a coil in air and saltwater. The red solid lines (-) are the inductance of a coil in air given by Grover's equation. The dashed lines (-) in blue are the inductances of the coil in seawater.

3. DESIGN OF RF COILS

Many different RF coils were investigated to determine the topologies best suited for integration into unmanned vehicles. Short, tightly wound cylindrical coils were designed with 18 AWG wire gauge, $N = 18$ turns, and radius $a = 6.0325$ cm. This diameter of the coils and number of turns met the spacing requirement for a UUV. The estimated inductance based on these parameter values was 80 μ H. To achieve the desired frequency of operation at 100 KHz, a $C = 33$ -nF capacitor was placed in series with the coil. The designed coils needed to be potted to protect the copper wire from the saltwater environment. A clear urethane potting material, previously used on hydrophones with a permeability of 1, was used as the potting material. A thermal epoxy was also applied to the coil to aid in

dissipating the thermal load from the applied current. An example of one of the tethered cylindrical coils is shown in the Figure 5(a).

Solenoid coils were also designed and fabricated. The receive coil was designed to be inserted inside the transmit coil, as shown in Figure 5(b). The receive coil was filled with a ferrite powder to increase its inductance and weight. The transmit coil was a tightly wound, single-layer solenoid with a 5.715-cm diameter, length of 2.54 cm, and 16 turns of 18 AWG 100-Khz Litz wire. The calculated inductance for the transmit coil with these dimensions was 46.5 μ H, and using an LCR meter, the measured inductance was 53 μ H. The receive coil's radius was slightly smaller and had eight turns of 18 AWG 100-Khz Litz wire. Its measured inductance was 9 μ H when filled with air. Both transmit and receive solenoids were potted. The receive coil was potted with iron powder to add weight when submerged underwater.

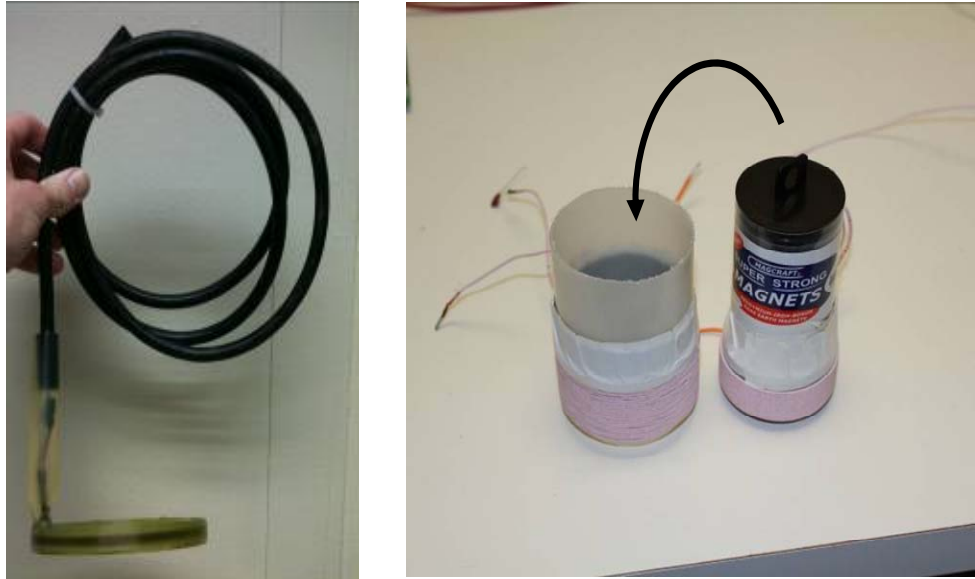


Figure 5. a) Tethered circular coil (left), and b) solenoid coils (right).

4. INPUT IMPEDANCE MEASUREMENTS

Input impedance measurements were conducted to characterize the various coil designs. Single-coil measurements were performed on the un-potted, potted, and coated coils to understand whether the potting process would change the impedance or add any additional loss into the system. Figure 6 shows the experimental setup for the input impedance measurements in seawater. The S-parameters were first measured using an Agilent E5071C network analyzer. The measurements were performed from 10 kHz to 1 MHz. The S-parameters were then converted to input impedance using the formula,

$$Z_{in} = Z_o \frac{1 - S_{11}}{1 + S_{11}},$$

where Z_o is 50 Ω . Once the input impedance was measured, the resistance and the inductance of the coil could be extracted from the real part of the impedance and its reactance.



Figure 6. Experimental setup for two-coil measurements in a seawater tank.

4.1 SINGLE-COIL MEASUREMENTS

Single-coil measurements were performed on the tethered circular coils and solenoids in air and in the saltwater aquarium. In air, the resistance of the circular coil was about $1\ \Omega$. The inductance in air for the different designed circular coils varied between 77 to $80\ \mu\text{H}$ around the operating frequency of $100\ \text{kHz}$. The tethered coil was then submerged into a tank of ocean saltwater. Figure 7 compares the resistance and reactance of the coils in air versus saltwater. The discrepancy between the two different mediums when operating below $100\ \text{kHz}$ was small. Above this frequency, the resistance of the coil in seawater begins to increase. Also shown is a result for a coil placed on top of a ferrite plate. In comparison, the coil placed on the ferrite plate resulted in much higher reactance and the resistance compared to the coil in air.

The quality factor, Q , can be determined from the measured resistance and inductance of each coil,

$$Q = \frac{\omega L}{R_{Tot}}.$$

The Q for the different coil configuration is shown in Figure 8. The higher resistance from the coil in seawater diminished the Q of the coil significantly.

The input impedance for the single layer solenoid was measured next. Figure 9 shows a comparison of the resistance and inductance versus frequency for the transmit solenoid coil in air and saltwater. The resistance of the coil below the operating frequency of $100\ \text{kHz}$ was $0.25\ \Omega$ in air and in seawater. But above $100\ \text{kHz}$, the resistance of the coil in seawater increased rapidly with frequency. The reactance for the solenoid in air or seawater showed little variation. The coil was tuned to $100\ \text{kHz}$ with a capacitor value of $C = 47\ \text{nF}$.

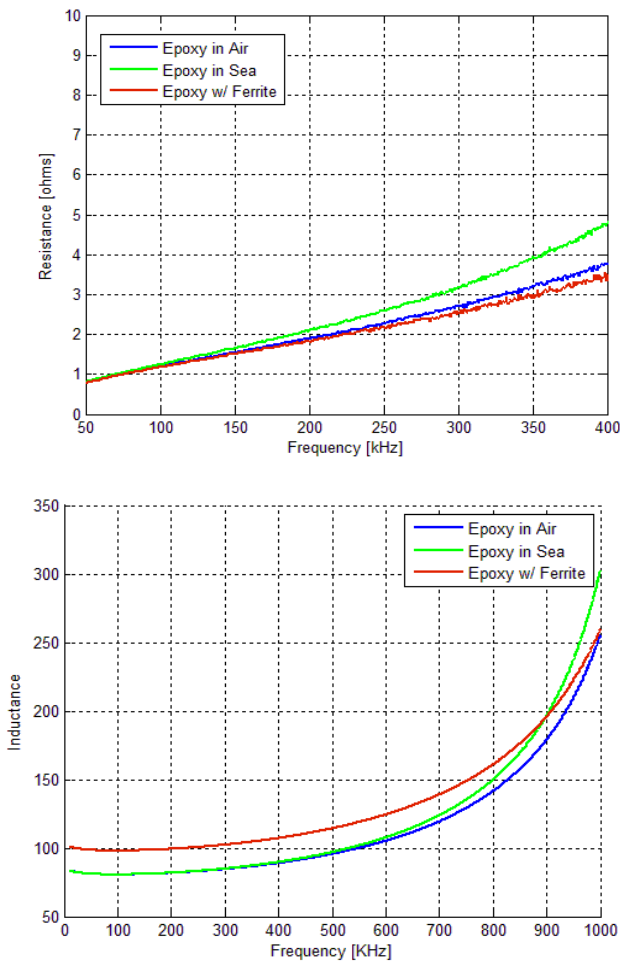


Figure 7. Input impedance measurements versus frequency for a single cylindrical coil in air and seawater, (a) resistance, and (b) reactance.

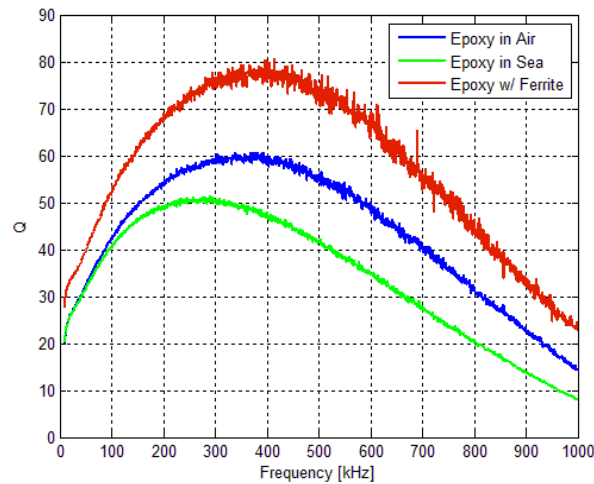


Figure 8. Quality factor of the coils in air, seawater, and atop a ferrite plate.

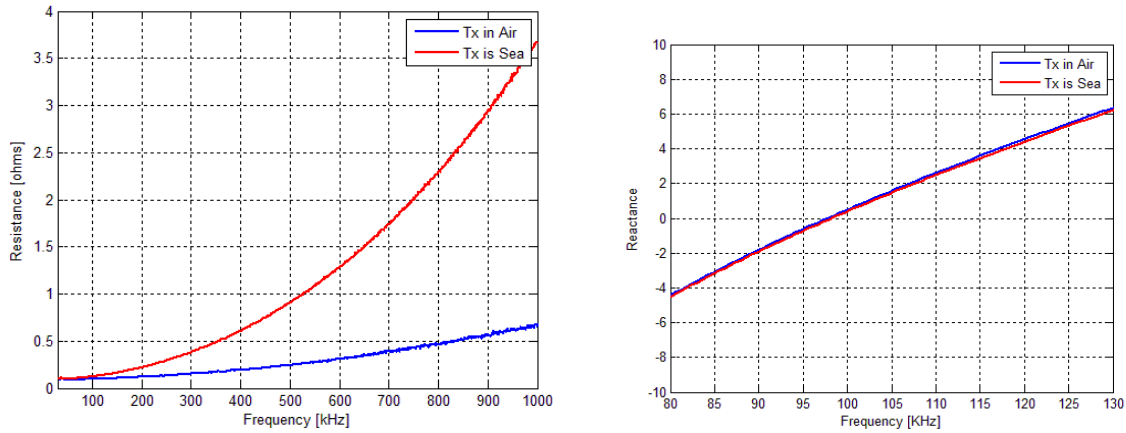


Figure 9. Input impedance measurement versus frequency for the transmit solenoid in air and seawater, (a) resistance, and (b) reactance.

4.2 COUPLED TWO-COIL MEASUREMENTS

Input measurements were performed on the coupled cylindrical coils and solenoids. For both cases, the load was a 1- Ω resistor. Both sets of coils were tuned to 100 kHz. For the cylindrical coils, the spatial separation varied from 2.54 to 20.32 cm. Figure 10 shows a comparison between the two-coil systems in air and saltwater. For this work, the frequency range was around 100 kHz. There is little difference in input impedance between the coils operating in air or seawater. The resistance was as high as 200 Ω at resonance for 2.54-cm spacing and then quickly fell off to 20 Ω for 5.08-cm spacing. The reactance, however, shows much greater variability over the range of coil spacing.

Figure 11 shows the input impedance measurements versus frequency for the coupled solenoids in air and seawater. These coils were designed so that the receive coil would fit closely inside the transmit coil. The spacing between the two coils was on the order of millimeters. Again, near an operating frequency of 100 kHz, the two measurements in air and seawater are in good agreement. For frequencies greater than 300 kHz, the resistance increased for the coil in saltwater. In comparison, the variation in reactance was small, whether the coils were in air or seawater.

The final analysis of the electrical properties for the coupled coils was to provide an estimate of the separation coefficient k_{12} or mutual coupling between the coils. The separation coefficient is given by the expression,

$$k_{12} = \frac{M}{\sqrt{L_1 L_2}}.$$

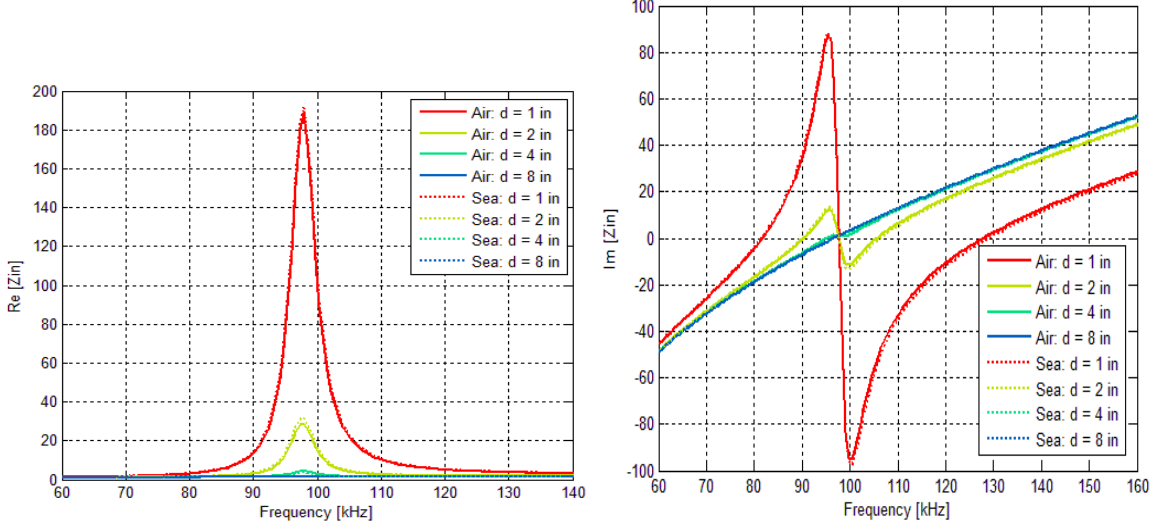


Figure 10. Comparison of the input impedance versus frequency for coupled cylindrical coils in air versus saltwater. Measurements are conducted for difference spacing between coils.

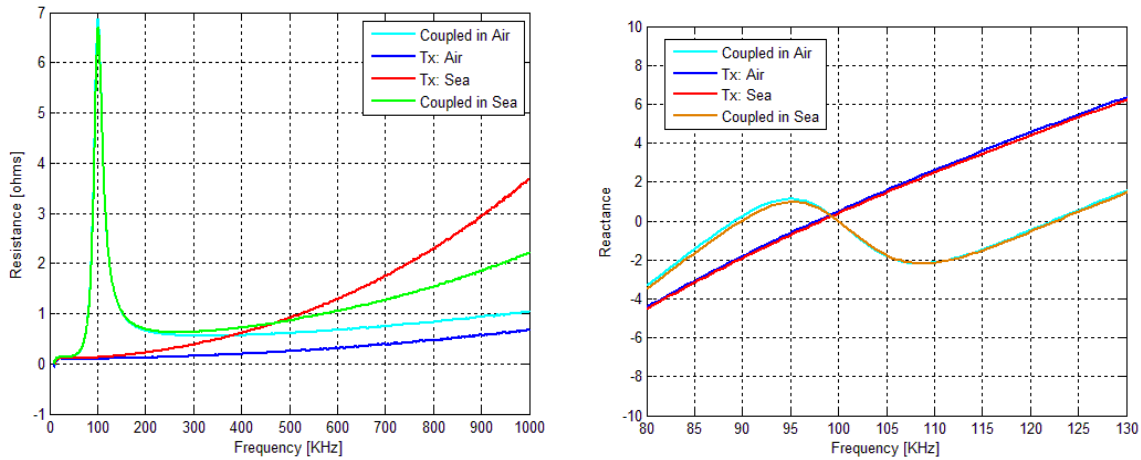


Figure 11. Comparison of the input impedance versus frequency for the coupled transmit and receive solenoid in air versus saltwater. Measurement was performed for the receive coil slotted inside the transmit coil.

The separation coefficient k_{12} can range in value from 1.0 (good coupling) to 0.0 (poor coupling). The k_{12} coefficient is extracted from the two-coil impedance measurements using the method described in [9]. Figure 12 is a summary of the estimated k_{12} versus spacing for the different designed coils setups. For the solenoids, where the receive coil fit snugly inside the transmit coil, the k_{12} value was approximately 0.7. The cylindrical coils k_{12} ranged from 0.4 to 0.15 for coil spacing. The solenoid coils appeared to provide better coupling. Therefore, two final coils were designed based on the transmit solenoid. The extracted k_{12} values for this final coupled solenoid are shown in green in Figure 12. They show slight improvement in k_{12} value over the cylindrical coils.

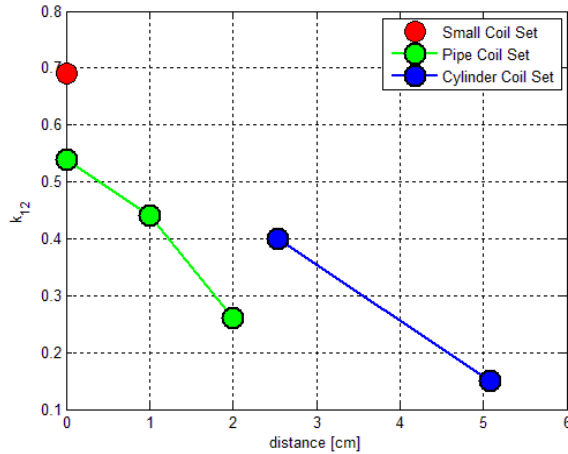


Figure 12. Separation coefficient for cylindrical coils ('blue'). quality factor of the coils in air, seawater, and atop a ferrite plate.

5. CONCLUSION

Using two-port network analysis, key parameters of an underwater wireless power system were measured. Preliminary results indicate that at frequencies below 100 kHz, the electrical properties of coils and their mutual coupling were almost identical, whether in air or in saltwater. Above 100 kHz, seawater began to have a detrimental effect on the resistance of the coil and their coupling performance. Future work will use coils made with larger and higher frequency Litz wire and increase the resonance frequency to determine when saltwater will affect the power transfer.

6. REFERENCES

- [1] A. Bradly, M. Freezor, H Singh, and F Sorrell. 2001. "Power Systems for Autonomous Underwater Vehicles," *IEEE Journal of Oceanic Engineering Conference on Mechatronics and Automation Changchun China*, vol. 26, no. 4, pp. 526–538 (October).
- [2] Q. Gau, X. Wu, J. Liu, and Z. Yang. 2009. "Modeling and Simulation of Contact-less Power Transformers for Underwater Applications," *IEEE Proceedings International Conference on Mechatronics and Automation Changchun China*, vol. 2, pp. 1213–1217 (August).
- [3] M. Dionigi, A. Costanzo, and M. Mongiardo. 2001. "Network Methods for Analysis and Design of Resonant Wireless Power Transfer Systems." In *Wireless Power Transfer-Principles and Engineering Explorations*, pp. 65–94, Dr. Ki Young Kim, Ed. In Tech , <http://www.intechopen.com>.
- [4] A. P. Sample, D. A. Meyer, and J. R. Smith. 2011. "Analysis, Experimental Results, and Range Adaptation of Magnetically Coupled Resonators for Wireless Power Transfer," *IEEE Transactions on Industrial Electronics*, vol. 58.2, pp. 544–554.
- [5] M. B. Kraichman. 1962. "Impedance of a Circular Loop in an Infinite Conducting Medium," *Journal of Research of the National Bureau of Standards, Section D. Radio Propagation*, vol. 66.4, 499–503.
- [6] D. M. Pozar. 1998. *Microwave Engineering*. 2nd ed. John Wiley & Sons, New York, NY.

- [7] F. W. Grover. 1946. *Inductance Calculations: Working Formulas and Tables*. D. Van Nostrand Company, Inc., New York, NY.
- [8] S. Babic, F. Sirois, C. Akyel, and C. Girardi. 2010. “Mutual Inductance Calculation Between Circular Filaments Arbitrarily Positioned in Space: Alternative to Grover’s Formula,” *IEEE Transactions on Magnetics*, vol. 46, no. 9 (September).
- [9] G. Hong and M. J. Lancaster. 2001. *Microstrip Filters for RF/Microwave Applications*. Chapter 8. John Wiley & Sons, New York NY.

INITIAL DISTRIBUTION

84300	Library	(2)
85300	Archive/Stock	(1)
56480	Viktor Bana	(1)

Defense Technical Information Center
Fort Belvoir, VA 22060-6218 (1)

Approved for public release.



SSC Pacific
San Diego, CA 92152-5001